



**HAL**  
open science

# Decrease in Seismic Velocity Observed Prior to the 2018 Eruption of Kīlauea Volcano With Ambient Seismic Noise Interferometry

G. Olivier, F. Brenguier, R. Carey, P. Okubo, C. Donaldson

► **To cite this version:**

G. Olivier, F. Brenguier, R. Carey, P. Okubo, C. Donaldson. Decrease in Seismic Velocity Observed Prior to the 2018 Eruption of Kīlauea Volcano With Ambient Seismic Noise Interferometry. *Geophysical Research Letters*, 2019, 46, pp.3734-3744. 10.1029/2018GL081609 . insu-03595787

**HAL Id: insu-03595787**

**<https://insu.hal.science/insu-03595787>**

Submitted on 3 Mar 2022

**HAL** is a multi-disciplinary open access archive for the deposit and dissemination of scientific research documents, whether they are published or not. The documents may come from teaching and research institutions in France or abroad, or from public or private research centers.

L'archive ouverte pluridisciplinaire **HAL**, est destinée au dépôt et à la diffusion de documents scientifiques de niveau recherche, publiés ou non, émanant des établissements d'enseignement et de recherche français ou étrangers, des laboratoires publics ou privés.

Copyright

# Geophysical Research Letters

## RESEARCH LETTER

10.1029/2018GL081609

### Key Points:

- We use ambient seismic noise interferometry to measure changes in seismic velocity at Kilauea during to the initiation of the 2018 eruption
- We detect a rapid seismic velocity decrease 10 days before the eruption
- This decrease is likely a result of damage accumulation in the edifice due to increased pressure

### Supporting Information:

- Supporting Information S1

### Correspondence to:

G. Olivier,  
 gjf.olivier@gmail.com

### Citation:

Olivier, G., Brenguier, F., Carey, R., Okubo, P., & Donaldson, C. (2019). Decrease in seismic velocity observed prior to the 2018 eruption of Kilauea volcano with ambient seismic noise interferometry. *Geophysical Research Letters*, *46*, 3734–3744. <https://doi.org/10.1029/2018GL081609>

Received 10 DEC 2018

Accepted 22 MAR 2019

Accepted article online 28 MAR 2019

Published online 8 APR 2019

## Decrease in Seismic Velocity Observed Prior to the 2018 Eruption of Kilauea Volcano With Ambient Seismic Noise Interferometry

G. Olivier<sup>1,2,3</sup> , F. Brenguier<sup>1</sup> , R. Carey<sup>2</sup>, P. Okubo<sup>4</sup>, and C. Donaldson<sup>5</sup> 

<sup>1</sup>Institut des Sciences de la Terre, Université Grenoble Alpes, CNRS, Grenoble, France, <sup>2</sup>CODES and School of Physical Sciences, University of Tasmania, Hobart, Tasmania, Australia, <sup>3</sup>Institute of Mine Seismology, Hobart, Tasmania, Australia, <sup>4</sup>Hawaiian Volcano Observatory, US Geological Survey, Hilo, HI, USA, <sup>5</sup>Bullard Laboratories, Department of Earth Sciences, University of Cambridge, Cambridge, UK

**Abstract** The 2018 Kilauea eruption was a complex event that included deformation and eruption at the summit and along the East Rift Zone. We use ambient seismic noise interferometry to measure time-lapse changes in seismic velocity of the volcanic edifice prior to the lower East Rift Zone eruption. Our results show that seismic velocities increase in relation to gradual inflation of the edifice between 1 March and 20 April. In the 10 days prior to the 3rd of May eruption onset, a rapid seismic velocity decrease occurs even though the summit is still inflating. We confirm that intereruptive velocity change is correlated with surface deformation, while the velocity decrease prior to eruption is likely due to accumulating damage induced by the pressure exerted by the magma reservoir on the edifice. The accumulating damage and subsequent decrease in bulk edifice strength may have facilitated increased transport of magma from the summit reservoir to the Middle East Rift Zone.

### 1. Introduction

Volcanic eruptions occur, generally, when pressure within the magma reservoir exceeds the strength of the confining, surrounding rock mass (Blake, 1984; Gerbault et al., 2012; Gudmundsson, 2006; McLeod & Tait, 1999; Tait et al., 1989). As the pressure builds, eruptions are often preceded by an increase in seismic activity and surface deformation, which are often reliable indicators of impending eruption (Budi-Santoso et al., 2013; Kilburn, 2003, 2012; Lengliné et al., 2008; Peltier & Bachèlery, 2009; Peltier et al., 2005, 2006; Schmid et al., 2012; Surono et al., 2012; Voight, 1988). However, abrupt increases in seismic activity or surface deformation at Kilauea are not always indicative of an impending eruption and may occur due to intrusions of magma (Judson et al., 2018) or due to episodic deflation/inflation events (Anderson et al., 2015). This makes forecasting eruptions with surface deformation and seismic approaches alone challenging.

An eruption in the lower East Rift Zone (LERZ) of Kilauea Volcano started at roughly 17:00 on the 3rd of May 2018 (HST; Neal et al., 2019). Based on the rapid draining of magma at Pu'u 'Ō'ō coupled with extensional deformation and increased seismicity propagating to the LERZ, the Hawaiian Volcano Observatory issued a Volcano warning on 1 May about the possibility of an East Rift Zone Eruption. The eruption was preceded by inflation at Kilauea volcano's summit and overflow of the Halema'uma'u lava lake on the 24th of April. Deflation of the summit and rapid draining of the lava lake began on 1 May. The eruption was partly fed by the central summit reservoirs roughly 40 km away from the flank (Neal et al., 2019). The LERZ-eruption finally came to a halt in early August, after emitting around 800 million cubic meters of lava and destroying more than 700 homes (Loomis, 2018; Neal et al., 2019).

The monitoring program maintained by the USGS Hawaiian Volcano Observatory at Kilauea volcano is one of the most technologically advanced networks in the world, consisting of a dense network of seismic stations, digital tiltmeters and GPS stations. Thus, this eruption provides an opportunity to study the behavior of the volcanic edifice prior to eruption and to improve our ability to predict similar eruptions elsewhere (e.g., Reardon, 2018). Ambient seismic noise interferometry has enabled geophysicists to monitor temporal variations in seismic wave speed with unprecedented precision. The method has shown particular promise in monitoring changes in seismic velocity at volcanoes prior to eruptions (e.g., Brenguier et al., 2008). However, the causes of these pre-eruptive changes are not well understood. In this paper, we examine whether

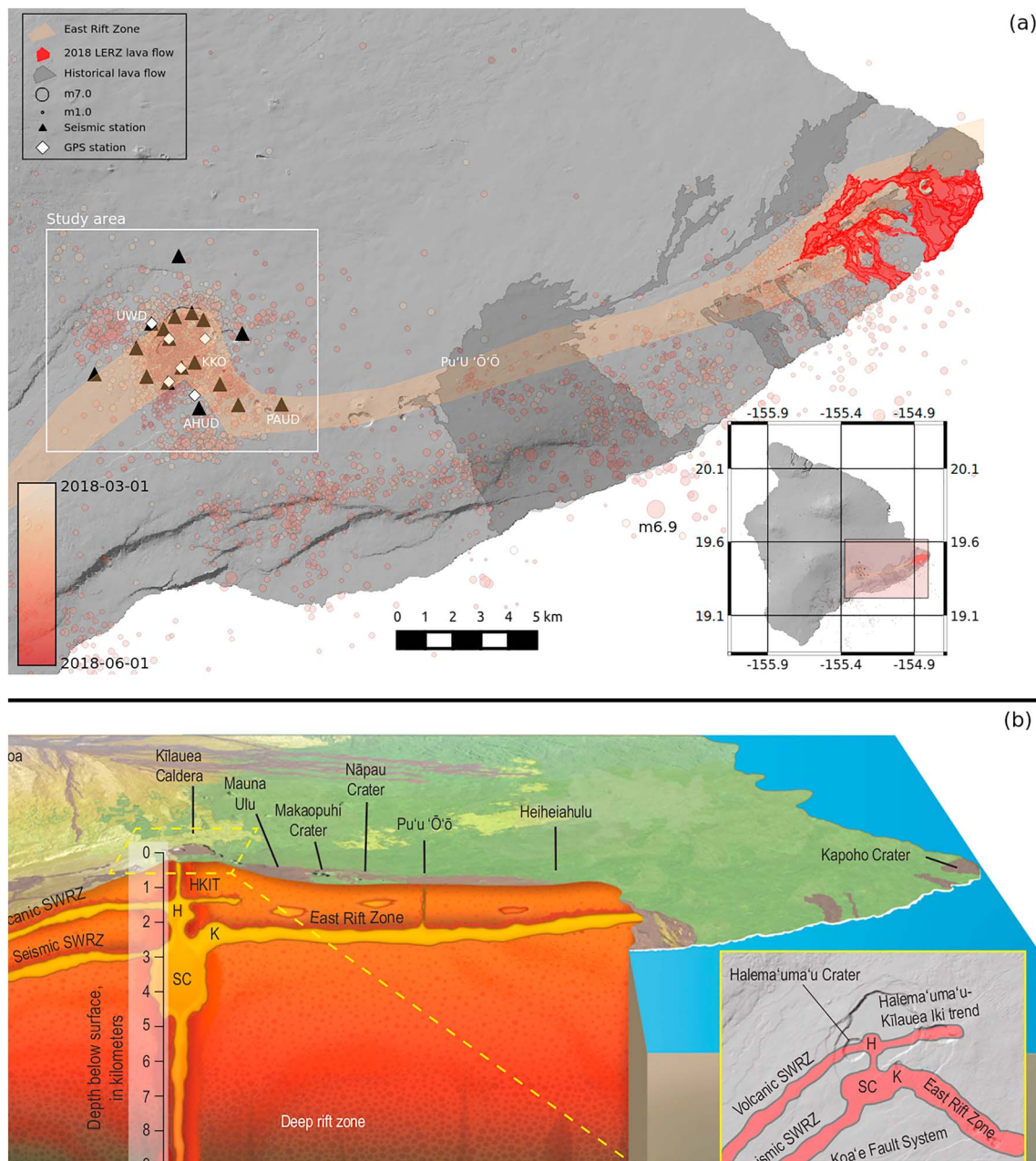


**Figure 1.** Geophysical Network and Setting. (a) Locations of the summit seismic, GPS, and tilt stations used in this study. The locations of the seismic events recorded in the same time period is shown as spheres colored by time and sized by magnitude. The locations of the SW and East Rift Zones and selected historical lava flows are also indicated. (b) Illustration of the plumbing system of the Kilauea volcano from Poland et al. (2014). The Halema'uma'u reservoir (H) and the South Caldera reservoir (SC) are shown along with the connection to the East Rift Zone. The size of magma pathways and storage are exaggerated here for clarity. LERZ = Lower East Rift Zone.

changes in seismic velocity measured with ambient seismic noise can provide insights into the physical processes that were a prelude to the onset of the Kilauea eruption. Even though the majority of the destruction occurred roughly 40 km away from the summit, the central summit reservoirs feed the various magma conduits such as the East Rift Zone. As a result most of our research is focused around the behavior of the summit edifice.

## 2. Methods

Over the last decade a new method, called ambient seismic noise interferometry, has enabled geophysicists to monitor temporal variations in seismic wave speed with unprecedented precision. Ambient noise studies

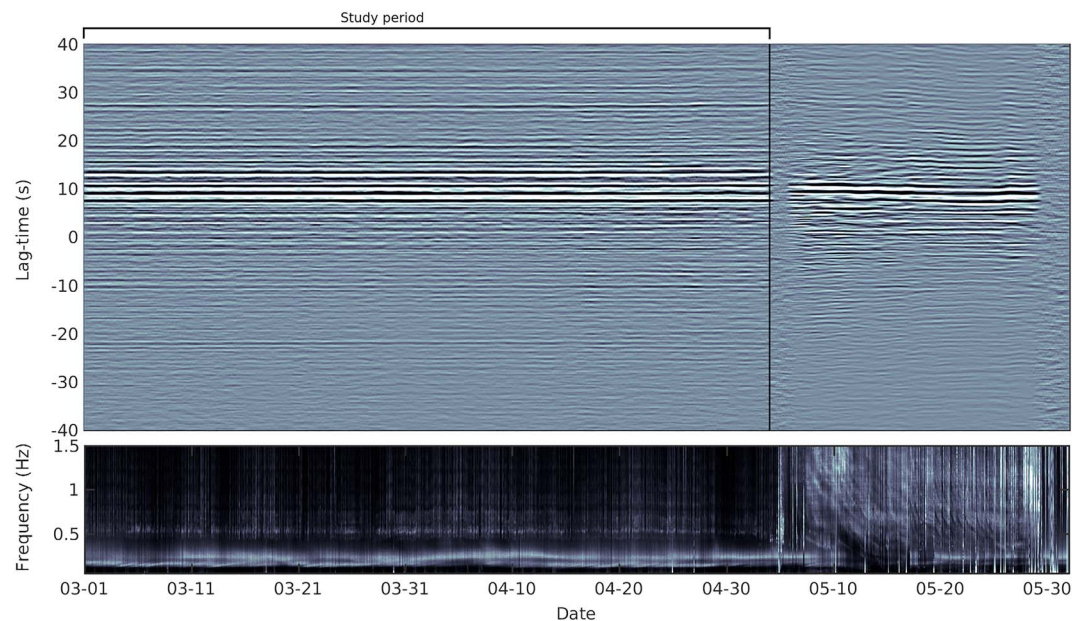


**Figure 2.** Hourly cross-correlation functions for E components of stations PAUD and KKO stations (top) and stacked hourly spectra for all considered station components (bottom). The black line indicates the onset of the eruption on the 3rd of May at 17:00 (HST). A 24-hr moving average was applied to both. The cross-correlation functions and stacked spectra are remarkably stable prior to the eruption. The locations of these two stations are indicated in Figure 1.

do not require an active source or repeating earthquakes and have been successfully applied to measure changes in seismic velocity in a range of different environments, such as volcanoes (Brenquier et al., 2008; Donaldson et al., 2017; Sánchez-Pastor et al., 2018; Sens-Schönfelder & Wegler, 2006), landslides (Mainsant et al., 2012), underground mines (Olivier et al., 2015), geothermal reservoirs (Hillers et al., 2015; Obermann et al., 2015), active faults zones (Brenquier et al., 2008), earthen dams (Olivier et al., 2017; Planès et al., 2015), and other environments. Ambient noise seismic interferometry typically refers to the cross-correlation of continuously recorded seismograms to construct virtual source signals between sensor pairs (Curtis et al., 2006). These virtual source signals can be constructed at different times, so small temporal changes in seismic velocity can be measured to study processes in the Earth's crust. Notably, it has been shown that a detectable change in seismic velocity occurs in the days leading up to an eruption at some volcanoes (Bennington et al., 2015; Brenquier et al., 2008; Budi-Santoso & Lesage, 2016; Caudron et al., 2015; Grêt et al., 2005; Hirose et al., 2017; Patanè et al., 2006; Ratdomopurbo & Poupinet, 1995; Wegler et al., 2006). Authors in these studies attribute precursory velocity changes to the dilation/compression of the edifice due to the increased pressure the magma chamber exerts on the edifice, which has been shown to cause measurable changes in seismic velocities at volcanoes (Sens-Schönfelder et al., 2014). The sign of the velocity change (increase or decrease) depends on topography and depth of the magma chamber relative to the seismic stations.

Continuous seismic data for 19 seismic stations around Halema'uma'u Crater (see Figure 1) from the 1st of March until the 1st of June was divided in 30-min segments, one-bit normalized and spectrally whitened between 0.08 and 2 Hz. These segments were then cross-correlated between station pairs and stacked to create daily cross-correlation functions for each station pair. Cross-correlation functions were created between all station components, but components that produced correlations functions with poor signal-to-noise ratios were removed (see supporting information for details). Single-station cross-component correlations were also included in the analysis, but autocorrelations were not considered for this study. This resulted in 820 correlation pairs.

Figure 2 shows the hourly cross-correlation functions for stations PAUD and KKO, along with the hourly stack of the power-spectral densities for all considered station components (both smoothed by 24-hr moving window). The spectral content shows the stable secondary oceanic microseism between 0.1 and 0.2 Hz along with the volcanic tremor between 0.3 and 1 Hz. The cross-correlation functions and hourly stacked power spectral densities are remarkably stable leading up to the eruption at roughly 17:00 (HST) on the 4th of May.

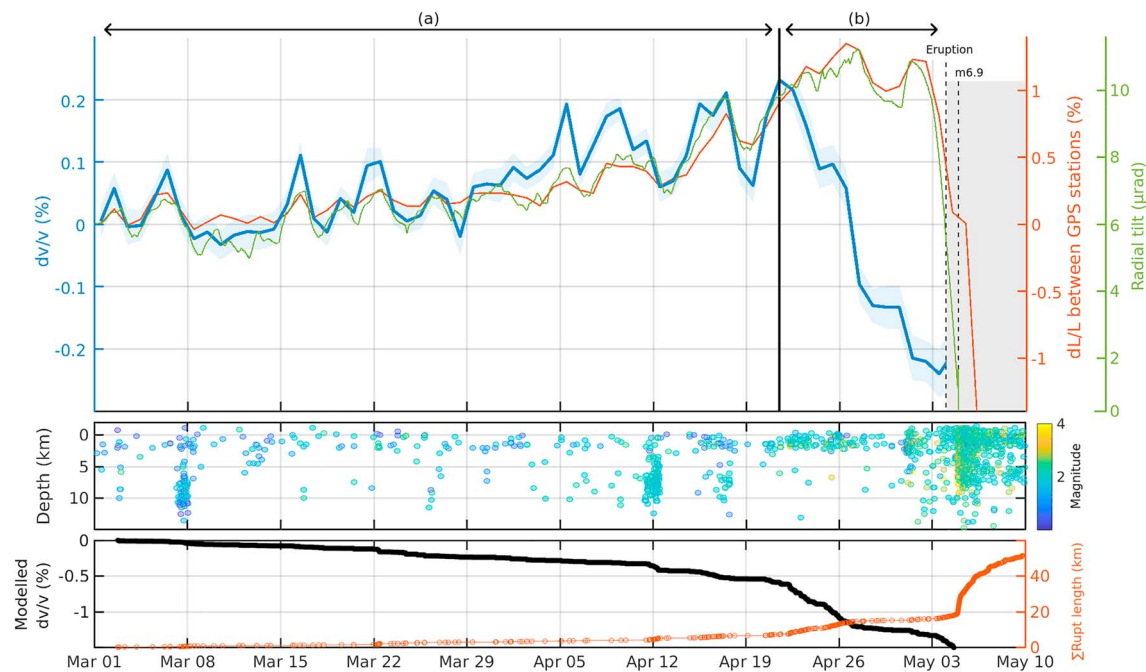


**Figure 3.** Average relative daily velocity changes (blue) compared to relative change in baseline distance averaged for all GPS stations crossing the caldera (red) and radial tilt measured at station UWD (green). The blue shaded area indicates the uncertainty in the relative velocity change measurements. The velocity changes are well correlated with relative distance and radial tilt change up to the 20th of April, after which there is rapid decrease in velocity even though inflation is still being registered by the GPS and tilt stations. The gray area indicates the period when the cross-correlation functions become too unstable for reliable measurements. In the middle panel, all recorded seismic events are shown. There is a swarm of seismic events in the summit region in the days leading up to the eruption. The bottom panel shows the cumulative rupture length and the modeled velocity decrease due to the damage accumulation from earthquakes. See the Acknowledgments section for information on data availability.

After the eruption, there is a clear increase in seismic energy at higher frequencies due to the increased seismic activity induced by the eruption and draining of the lava lake. As a result the cross-correlation functions become less stable. This effect was observed for all station pairs (see supporting information for details).

Daily velocity variations were computed with the moving window cross-spectral technique (Clarke et al., 2011) for all station pairs and averaged. Velocity changes were measured in the frequency band 0.08 to 1.2 Hz and in 30-s windows in the causal and acausal section of the coda of the surface wave arrivals (calculated as the distance between stations divided by 700 m/s plus 30 s). By only measuring changes in the coda, we reduce the influence of changing noise source locations and frequency content (Hadziioannou et al., 2009). Since the multiply scattered waves that make up the coda of the waveforms sample the medium for longer time, they are also more sensitive to subtle changes in the medium. Surface wave speeds of approximately 1 km/s result in the measurements being mostly sensitive to changes between 250 m and 4 km depths (see supporting information). This band was chosen to include the effects of the South Caldera (deep) and the Halema'uma'u (shallow) magma reservoirs on the seismic velocity measurements (Poland et al., 2014).

The velocity variations were compared to the geodetic line-length changes between GPS stations around the summit, radial tilt, and the seismic activity (see Figure 3). From the 1st of March to the 21st of April there is a clear positive correlation between the seismic velocity changes, GPS line-length, and radial tilt (Pearson correlation coefficient of 0.86 and 0.9, respectively). The gradual increase in distance between the GPS stations and radial tilt results from inflation of the summit in response to increased pressure of the magma chamber(s) (Neal et al., 2019). The increase in velocity is due to the increase in pressure of the medium between the magma chamber and the surface and is consistent with recent observations from Donaldson et al. (2017).

From the 21st of April to the 1st of May, there is a rapid decrease in velocity despite continued gradual inflation observed at the summit. Remarkably there are little other geophysical indication of instability at the summit during this time period (see chronology of events from USGS in the supporting information S2

and Neal et al., 2019). This observation indicates that a secondary process is driving velocity changes during this time that is not discernible by measurements of surface deformation or other monitored parameter.

Due to the increase in seismic and volcanic activity at the summit after the 3rd of May, the correlation functions become incoherent, resulting in large uncertainty in the velocity change measurements (indicated by the large uncertainties in the measurements in Figure 3 and the loss of coherence in the CCFs in Figure S2). As a result we refrain from interpreting the relative velocity variations after the onset of eruption.

### 3. Discussion

Two competing effects control seismic velocity changes observed at the summit of Kīlauea volcano prior to the eruption. These effects are indicated in Figure 3 as regions (a) and (b). First, region (a) shows an increase in seismic velocity while GPS line-length increases and the summit inflates. We interpret this as a response to increased pressure in the shallow magma chamber results in an increase in seismic velocity due to compression of most of the volcanic edifice between the 1st of March and the 19th of April. This effect has also been shown by a correlation between radial tilt and seismic velocity in the short-term (over days and weeks) between 2011 and 2015 (Donaldson et al., 2017). These authors proposed that increased pressure in the Halema'uma'u reservoir results in compression over most of the volcanic edifice, causing the closing of microcracks and hence an increase in seismic velocity. We suggest that this effect is still occurring during 1 March to 19 April, as the summit pressurizes.

The second effect, region (b), shows a rapid decrease in seismic velocity roughly 10 days prior to the eruption even though GPS line-length stays high and the summit remains inflated. There are two possible explanations for the observed velocity decrease. First, the velocity decrease could indicate the rapid pressurization of the deeper, South Caldera reservoir, which will cause overall dilation of the edifice and would subsequently cause the seismic velocity to decrease. Another possible explanation for the sudden decrease in seismic velocity prior to the eruption is accumulating damage and weakening of the edifice by the pressure exerted by the South Caldera and/or Halema'uma'u reservoir. To examine which of these effects are more likely to be responsible for the velocity decrease, we build on previous work that has examined these two driving forces at volcanoes (Carrier et al., 2015; Donaldson et al., 2017).

#### 3.1. Pressurization of the South Caldera Reservoir

The first potential mechanism we investigate builds on the existing model of intereruptive periods, where seismic velocity changes are linearly proportionate to strain changes (linear elastic regime).

Donaldson et al. (2017) showed that the long-term (months to years) trend in seismic velocity observed at Kīlauea was anticorrelated with tilt measured at surface. They postulated a secondary driving factor: these changes could be driven by pressure increase in the South Caldera reservoir, at 3–5 km depth (Poland et al., 2014), which would cause overall dilation of the volcanic edifice and velocity decrease. Bearing this in mind, the rapid velocity decrease starting on 21 April, roughly 10 days prior to the eruption (even while the summit is experiencing inflation) in the blue shaded area marked as (b) in Figure 3 could be indicative of a rapid increase in magma pressure in the deeper (South Caldera) reservoir. Further possible evidence of this phenomenon can be seen in the bottom of Figure 3. Here three periods of increased seismic activity can be seen at a depth of between 5 and 10 km below surface (7 March, 11 April, and 17 April). This increase in seismicity below the South Caldera reservoir could indicate infiltration of magma, which would in turn cause pressurization of the South Caldera reservoir.

To test whether pressurization of the South Caldera reservoir could produce the velocity decrease we observe prior to the eruption, we revisit the elastic strain model used by Donaldson et al. (2017). A more detailed discussion of the methodology can be found in the supporting information (Herrmann, 2013; Klein, 1981; Olivier et al., 2015; Toda et al., 2011). First, we develop the intereruptive case, when the shallow Halema'uma'u reservoir is likely responsible for the observed measurements of relative velocity variations. We model this reservoir as a pressurizing point source at 1.5 km depth below surface (Anderson et al., 2015). As shown by Donaldson et al. (2017), and also visible in the period before the 20th of April 2018 in this study,  $dv/v$  is positive correlated with inflation during large deflation-inflation (DI) events, and changes are on the order 0.1%. We use a volume change of  $3 \times 10^5 \text{ m}^3$ , corresponding to the volume change in the Halema'uma'u

reservoir during large DI events (Anderson et al., 2015) to get an estimate of the strain change induced by these DI events.

To get a reasonable estimate of the velocity-strain sensitivity, we calculate the effective strain by performing a weighted average of the strain as a function of depth, with the depth sensitivity kernels for Rayleigh waves in the frequency bands of interest providing the weighting factor at each depth (see supporting information for more detail). We use strain as a function of depth calculated at 3 km radial distance from the point source, as this corresponds to the average station distance from the summit lava lake. The resulting volumetric strain for a large inflation event is  $-0.4$  microstrain (compression). This in turn corresponds to a velocity-strain sensitivity of 0.25% per microstrain, which compares well with results from literature for other environments (e.g., Mordret et al., 2016).

We then consider the 10-day pre-eruptive period, when  $dv/v$  decreases (Figure 3 marked as b). We suggest that the South Caldera reservoir is pressurizing at this time, while a blockage prevents further pressurization of the Halema'uma'u reservoir. Although this constraint is speculative, it provides the only conceivable mechanism for the decrease in velocity before the eruption for an elastic model. Therefore, we can model this as a deeper point source at 4 km depth (Anderson et al., 2015). The pre-eruptive decrease in  $dv/v$  we observe is 0.4%. Assuming the velocity strain sensitivity found during intereruptive periods, we would need the strain change produced by the South Caldera reservoir to be more than  $+1.4$  microstrain at a radial distance of 3 km from the Halema'uma'u reservoir. This in turn would require a volume change of  $8 \times 10^6$  m<sup>3</sup> in the South Caldera reservoir, which is roughly 1% of the estimated total erupted volume of the 2018 LERZ eruption (Neal et al., 2019). Such a rapid volume change at the South Caldera reservoir in a 10-day period of time is unlikely, as it would require the magma supply to the South Caldera reservoir to be more than three times higher than the long-term rate (Neal et al., 2019), even when assuming no magma loss to the Halema'uma'u reservoir or the East Rift Zone. Further, the rapid volume change of  $8 \times 10^6$  m<sup>3</sup> in the South Caldera reservoir would cause significant uplift at the locations of the GPS stations (more than 10 cm). However, the vertical displacements measured by the GPS stations only show uplift between 1 and 2 cm and no clear acceleration during the period where we observe a velocity decrease (see Figure S4). The lack of uplift could be explained if the pressure of the Halema'uma'u reservoir is simultaneously decreasing, counteracting the majority of inflation, but this is unlikely given that the lava lake level did not drop during this period. Therefore the pre-eruptive velocity decrease we observe is not likely driven by an increase in pressure in the South Caldera reservoir.

### 3.2. Damage Accumulation

The second possible explanation for the sudden decrease in seismic velocity prior to the eruption is accumulating damage and weakening of the edifice by the pressure exerted by the South Caldera and/or Halema'uma'u reservoir (nonlinear regime). Volcanic eruptions occur when the buildup of pressure in the magma reservoir exceeds the strength of the surrounding rock mass in the volcanic edifice, often resulting in increased seismic activity. Therefore, the precursory decrease in velocity could be driven by the nonlinear behavior of seismic velocity to increase in pressure from the South Caldera and/or Halema'uma'u reservoir that causes movement along grain boundaries, particle rolling and microcracking. This behavior was recently shown to be present prior to the full spectrum of earthquake failure modes in a laboratory study (Scuderi et al., 2016) and has also been proposed by other authors as a mechanism for velocity decrease prior to eruptions at volcanoes (Carrier et al., 2015; Rivet et al., 2014). In Figure 4 we show the spatial distribution of seismic velocity changes for three time periods prior to the eruption (top). In the figure we also show earthquake activity recorded since the 19th of April between surface and 4 km depth (top) and the velocity changes estimated at each station location (bottom). See supporting information for the method that is used to estimate the velocity changes at each station.

On the 21st of April (A), we see that the velocity increase is the highest just to the north of the Halema'uma'u Crater. We also note that some relatively shallow earthquakes during this period are located toward the East Rift Zone and that the velocity increase in this region is moderate compared to the rest of the summit. On the 27th of April (B), a noticeable velocity decrease has been detected in the region roughly 4 km southeast of the summit caldera toward the East Rift Zone. This velocity decrease is spatially correlated with clusters of seismic events with magnitude between M1.0 and M4.0. The spatial correlation between velocity decrease and seismic activity could be indicative of the damage-driven model of velocity decrease. Finally, on the 1st of May (two days before the eruption) (C) most of summit experiences a velocity decrease, apart from

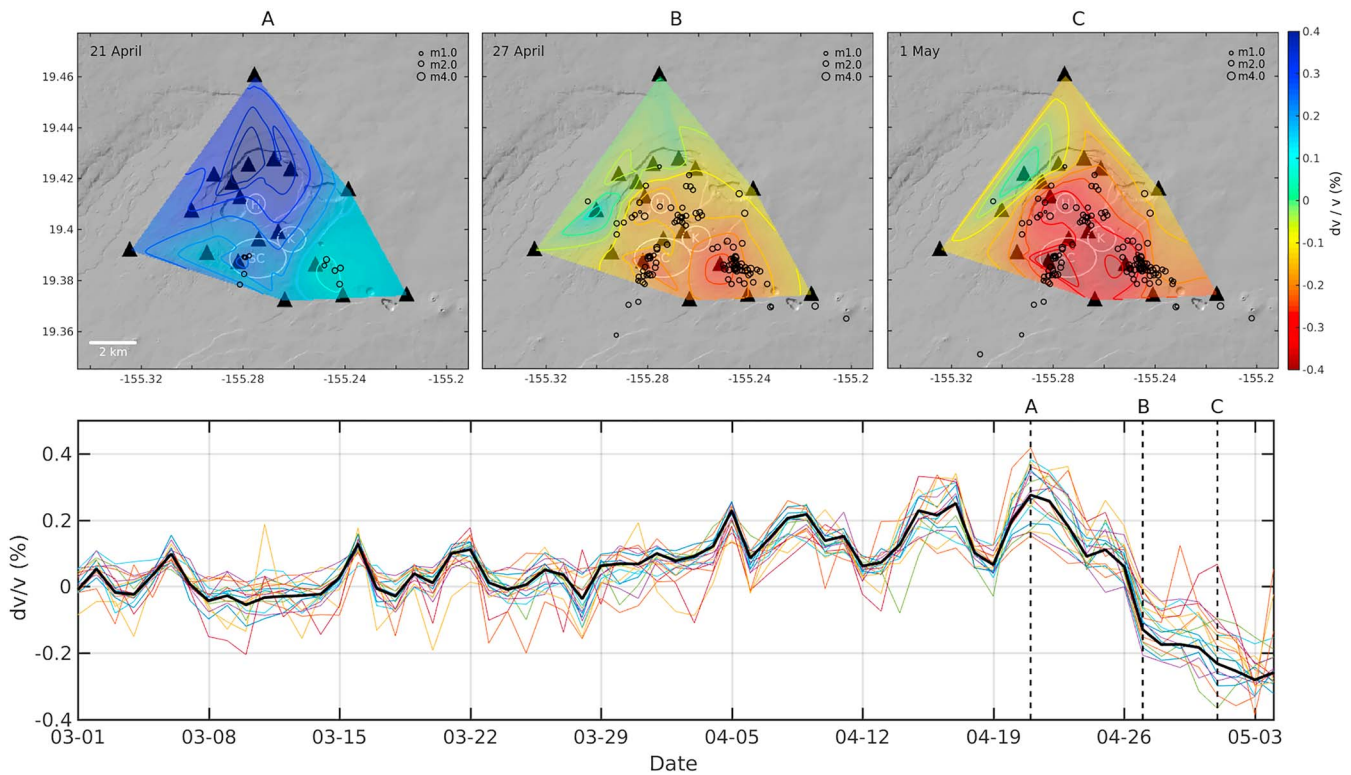


**Figure 4.** Spatial distribution of velocity changes for three time periods before the eruption along with earthquakes recorded during the same time period (top) inside the study area marked in Figure 1. The spatial distribution of the precursory velocity changes (B and C) are correlated with earthquakes roughly 4 km southeast of the caldera toward the East Rift Zone. The velocity changes estimated for each station location along with the average for the entire network (bottom). See supporting information for details on how these curves are produced.

the stations to the north west of the summit. This measurement represents velocity changes roughly a day before the increase in seismic activity and rapid deflation at the summit and the onset of the LERZ eruption (see Figure 3).

To test whether progressive damage of the edifice could explain the velocity decrease we observe, we implement a simple damage model as described in Carrier et al. (2015). We used a progressive homogeneous isotropic damage approach in order to link seismicity to the progressive failure of the edifice due to strain weakening and the subsequent decrease in seismic velocity before failure. Damage was introduced into the model by reducing the elastic shear modulus, using the seismicity rate (within the study region marked in Figure 1 up to 4 km below surface) and characteristic rupture length as a damage parameter. Similar to the approach of Carrier et al. (2015), we assume that the healing processes are slower than the damage processes and as a result this model can only account for a velocity decrease and can not replicate a velocity increase.

The characteristic rupture length for each event inside the volume where we measure seismic velocity variations was calculated from the scaling law  $A = 10^{0.82M - 2.87}$  (Wells & Coppersmith, 1994). The effective shear modulus of the edifice is then calculated as  $G' = (1 - D)G$ , where  $G$  is the initial shear modulus and  $D$  is the proportion of the damaged area. Therefore, damage decreases the elastic moduli of the initially perfectly elastic material. The change in  $S$  wave velocity due to the change in shear modulus is then  $dv/v = \sqrt{1 - D} - 1$ .

In Figure 3 we show the cumulative rupture length and modeled change in  $S$  wave velocity as a result of the progressive damage in the bottom panel (assuming a constant pressure and no healing) compared to the measured velocity changes in the top panel. We note that prior to the eruption there is a poor correlation between the modeled velocity decrease and the measured velocity change. This is likely because the model does not account for healing between successive seismic events and does not account for the pressure increase in the edifice. We do however see that the rapid decrease in velocity observed from the 19th of April until the 3rd of May is well reconstructed by the damage model where we measure a decrease of 0.4%, whereas the model predicts a decrease of 0.7%. We applied the same process to the stations around the Pu'u



'Ō'ō crater and found that the sudden decrease in velocity due to the crater collapse is also well described by the damage model (see supporting information).

The overestimation of the velocity changes by the damage model may be due to the overestimation of the rupture length of the earthquakes, since a simple scaling law was used as not an actual spectral fit for each earthquake. Another potential reason for the overestimation of the model is the assumption that each earthquake causes a decrease in the shear modulus of the edifice. Laboratory experiments have shown that a certain level of dynamic strain is required before a decrease in the shear modulus is observed (Johnson & Jia, 2005). This may indicate that some of the smaller magnitude earthquakes do not contribute to the decrease in shear modulus and therefore seismic velocity. Further improvements of the correlation of the modeled and the measured velocity variations could be made by including the linear elastic effects of inflation (and velocity increase) in the modeled velocity variations, since these effects have been observed and calibrated. However, since the correlation of the modeled and the measured velocity changes is intended to be qualitative and not quantitative, we did not attempt to modify the damage model to fit the observed data any further.

As well as explaining the observed velocity decrease prior to the eruption, the damage model can also provide a mechanism for the initiation of the LERZ eruption. The relative velocity variations (and the implementation of a cumulative damage model) indicate progressive damage in the region connecting the summit reservoir and the ERZ. This damage in turn increases the permeability, which might have facilitated the transport of magma from the summit reservoir(s) toward the East Rift Zone, causing the pressurization and inflation of the Halema'uma'u reservoir to slow and eventually leading to the summit collapse and draining of the Halema'uma'u reservoir from the 1st of May onward. A similar observation can be seen at Pu'u 'Ō'ō, where a sudden decrease in velocity is observed on 1 May (accompanied by damage), which precedes the dike infiltration and migration of magma down the LERZ (see Figures S6 and S7).

Further evidence that accumulating damage is the more likely mechanism of velocity decrease is the similarity of the  $dv/v$  measurements in different frequency bands (see Figure S1 and discussion). Measurements in the low frequency band sample much deeper and as a result would sample a large section of the compressive region if the deep source was pressurizing (see Figures S3 and S4). In other words, we expect that the low frequency band would see a much smaller pre-eruptive velocity decrease. The damage model on the other hand could explain the similarity by the relatively even distribution of earthquakes in the depth range which our measurements are sensitive to, indicating that the entire area we are probing is accumulating damage relatively evenly.

Accumulating damage in the edifice appears to be the most likely cause for the velocity decrease in the 10 days leading up to the eruption. However, it is possible that the decrease is driven by other effects. Below we mention a few possibilities and explain why these are unlikely.

### 3.3. Other Potential Mechanisms of Velocity Decrease

The decrease in velocity can also be induced by strong deformation from another source. The volcano's south flank moves seaward at a rate of around 8 cm/year and has generated several large earthquakes over the last 50 years (Owen et al., 2000). So far, no significant movement of the southern flank has been reported for the period between the 19th of April and the onset of eruption (the period where velocity decrease was detected). It is likely that deformation principally occurred at depth and that the lack of surface deformation does not rule out deeper displacements. Further investigation of gravity and surface displacement measurements could reveal the relationship between subsurface movement of the southern flank and the eruption, but at this stage there is no clear link.

Movement of the southern flank could explain the link between the volcanic eruption and the M6.9 earthquake that occurred shortly after eruption onset. Unfortunately due to the unstable nature of the correlation functions after the eruption commenced, it is hard for us to draw any conclusions on the effects of the M6.9 earthquake on the velocity changes in the volcanic edifice. However, other methods such as coda-wave interferometry of repeating earthquakes could potentially be used to study the behavior of the volcanic edifice during the eruption (Hotovec-Ellis et al., 2015).

Finally, the measured decrease in seismic velocity could be due to changes in the frequency content or location of the seismic noise sources (Zhan et al., 2013). Because the volcanic tremor is naturally linked to physical processes related to the eruption and is one of the dominant sources of noise (Ballmer et al., 2013),

this is a reasonable argument. However, the noise correlations (see Figure S2) and stacked spectra (Figure 2) indicated that there are no clear changes in either of these parameters during the time that the velocity decrease was detected. Furthermore, the volcanic tremor that is generated at the crater by the spluttering of the lava lake and the seismic activity produce frequencies larger than 0.5 Hz (see Figure 2 and Donaldson et al., 2017). Measurements in low frequency bands (0.08–0.2 Hz) show a very similar effect (see Figure S1), even though the noise in this band is dominated by the secondary oceanic microseism and the influence of change in the depth of the lava lake should be minimal in this band. The velocity decrease prior to eruption is also present at higher frequencies, which indicates that the measurements are likely due to actual changes in the medium rather than changes in noise sources. The coherence of the cross-correlation functions for all pairs leading up the eruption remain stable, which indicates that a change in the seismic noise source is not the likely cause for the velocity decrease.

### 3.4. Final Remarks

Ambient seismic noise interferometry is a promising method to monitor changes in seismic velocity to improve forecasting of volcanic eruptions. Recent work has shown a clear relationship between deformation and relative seismic velocity variations at Kīlauea summit during intereruptive periods (Donaldson et al., 2017). This study measures this correlation, but also reveals a fundamental shift in behavior for 10 days before the major 2018 eruption. Observing both these behaviors has enabled us to show that a secondary process is responsible for the pre-eruptive rapid decrease in seismic velocity. We examined the two most likely mechanisms of the velocity decrease and found that the velocity decrease is driven by accumulating damage of the edifice. The accumulating damage and subsequent decrease in bulk edifice strength likely facilitates the transport of magma from the summit reservoir to the East Rift Zone, potentially contributing to the ultimate initiation of the dike intrusion, Pu'u 'O'o collapse and the eruption in the LERZ.

The 2018 Kīlauea eruption has highlighted that our understanding of the physical processes responsible for eruptions needs to be improved. New methods such as seismic interferometry and improved measurements of surface deformation have enabled us to study volcanoes continuously over time and in great detail. The remarkable changes we observe around the central summit reservoirs that fed the eruption show that the method is robust and well suited for forecasting volcanic eruptions in conjunction with other observations. These observations will improve our understanding of the eruptive process and have direct implications for monitoring volcanoes for signs of impending eruption at Kīlauea, Piton de la Fournaise, and other similar volcanoes around the world.

### References

- Anderson, K. R., Poland, M. P., Johnson, J. H., & Miklius, A. (2015). Episodic deflation-inflation events at Kīlauea volcano and implications for the shallow magma system. *Hawaiian Volcanoes: From Source to Surface*, 208, 229–250.
- Ballmer, S., Wolfe, C. J., Okubo, P. G., Haney, M. M., & Thurber, C. H. (2013). Ambient seismic noise interferometry in Hawai'i reveals long-range observability of volcanic tremor. *Geophysical Journal International*, 194(1), 512–523.
- Bennington, N. L., Haney, M., De Angelis, S., Thurber, C. H., & Freymueller, J. (2015). Monitoring changes in seismic velocity related to an ongoing rapid inflation event at Okmok volcano, Alaska. *Journal of Geophysical Research: Solid Earth*, 120, 5664–5676. <https://doi.org/10.1002/2015JB011939>
- Blake, S. (1984). Volatile oversaturation during the evolution of silicic magma chambers as an eruption trigger. *Journal of Geophysical Research*, 89(B10), 8237–8244. <https://doi.org/10.1029/JB089iB10p08237>
- Brenguier, F., Campillo, M., Hadziioannou, C., Shapiro, N. M., Nadeau, R. M., & Larose, E. (2008). Postseismic relaxation along the San Andreas fault at Parkfield from continuous seismological observations. *Science*, 321, 1478–1481.
- Brenguier, F., Shapiro, N. M., Campillo, M., Ferrazzini, V., Duputel, Z., Coutant, O., & Nercessian, A. (2008). Towards forecasting volcanic eruptions using seismic noise. *Nature Geoscience*, 3(2), 126–130.
- Budi-Santoso, A., & Lesage, P. (2016). Velocity variations associated with the large 2010 eruption of Merapi volcano, Java, retrieved from seismic multiplets and ambient noise cross-correlation. *Geophysical Journal International*, 206(1), 221–240. <https://doi.org/10.1093/gji/ggw145>
- Budi-Santoso, A., Lesage, P., Dwiyo, S., Sumarti, S., Subandriyo, S., & Metaxian, J.-P. (2013). Analysis of the seismic activity associated with the 2010 eruption of Merapi Volcano, Java. *Journal of Volcanology and Geothermal Research*, 261, 153–170. <https://doi.org/10.1016/J.JVOLGEORES.2013.03.024>
- Carrier, A., Got, J.-L., Peltier, A., Ferrazzini, V., Staudacher, T., Kowalski, P., & Boissier, P. (2015). A damage model for volcanic edifices: Implications for edifice strength, magma pressure, and eruptive processes. *Journal of Geophysical Research: Solid Earth*, 120, 567–583. <https://doi.org/10.1002/2014JB011485>
- Caudron, C., Lecocq, T., Syahbana, D. K., McCausland, W., Watlet, A., Camelbeeck, T., & Suro, A. B. (2015). Stress and mass changes at a "wet" volcano: Example during the 2011–2012 volcanic unrest at Kawah Ijen volcano (Indonesia). *Journal of Geophysical Research: Solid Earth*, 120, 5117–5134. <https://doi.org/10.1002/2014JB011590>
- Clarke, D., Zaccarelli, L., Shapiro, N., & Brenguier, F. (2011). Assessment of resolution and accuracy of the moving window cross spectral technique for monitoring crustal temporal variations using ambient seismic noise. *Geophysical Journal International*, 136(5), 867–882.

### Acknowledgments

The authors thank the United States Geological Survey and the Hawaiian Volcano Observatory for the collection of all the data used in this study. The authors would like to thank Michael Poland, Alicia Hotovec-Ellis, Anne Obermann, and an anonymous reviewer for the useful discussions and feedback on the manuscript. We also thank Wes Thelen for providing radial tilt data. Funding: Funding for the research was provided by ISTerre. R. C. supported by the Australian Research Council grant DE150101190 and NSF EAR-1829188. C. D. received funding from a graduate studentship from the Natural Environment Research Council (NE/L002507/1) and Department of Earth Sciences, University of Cambridge. Author contributions: G. O. initiated the study, processed the data, interpreted the results, and wrote the manuscript. F. B. assisted with the data processing, interpretation, and preparation of the manuscript. C. D. conducted the strain modeling and assisted with the interpretation of the results and the preparation of the manuscript. R. C. and P. O. contributed to the interpretation of the results and the preparation of the manuscript. Competing interests: The authors declare that they have no competing interests. Data and materials availability: All data used to produce these results can be downloaded or requested. Continuous seismic data and earthquake catalog can be retrieved from the Incorporated Research Institutions for Seismology (<https://ds.iris.edu>). GPS data can be retrieved from UNAVCO ([www.unavco.org](http://www.unavco.org)). Radial tilt data were supplied by HVO.

- Curtis, A., Gerstoft, P., Sato, H., Snieder, R., & Wapenaar, K. (2006). Seismic interferometry—Turning noise into signal. *The Leading Edge*, 25(9), 1082–1092. <https://doi.org/10.1190/1.2349814>
- Donaldson, C., Caudron, C., Green, R. G., Thelen, W. A., & White, R. S. (2017). Relative seismic velocity variations correlate with deformation at Kilauea volcano. *Science Advances*, 6, e1700219. <https://doi.org/10.1126/sciadv.1700219>
- Gerbault, M., Cappa, F., & Hassani, R. (2012). Elasto-plastic and hydromechanical models of failure around an infinitely long magma chamber. *Geochemistry, Geophysics, Geosystems*, 13, Q03009. <https://doi.org/10.1029/2011GC003917>
- Grêt, A., Snieder, R., Aster, R. C., & Kyle, P. R. (2005). Monitoring rapid temporal change in a volcano with coda wave interferometry. *Geophysical Research Letters*, 32, L06304. <https://doi.org/10.1029/2004GL021143>
- Gudmundsson, A. (2006). How local stresses control magma-chamber ruptures, dyke injections, and eruptions in composite volcanoes. *Earth-Science Reviews*, 79(1–2), 1–31. <https://doi.org/10.1016/j.earscirev.2006.06.006>
- Hadziioannou, C., Larose, E., Coutant, O., Roux, P., & Campillo, M. (2009). Stability of monitoring weak changes in multiply scattering media with ambient noise correlation: Laboratory experiments. *Journal of the Acoustical Society of America*, 125, 3688–3695.
- Herrmann, R. B. (2013). Computer programs in seismology: An evolving tool for instruction and research. *Seismological Research Letters*, 84(6), 1081–1088.
- Hillers, G., Husen, S., Obermann, A., Planès, T., Larose, E., & Campillo, M. (2015). Noise-based monitoring and imaging of aseismic transient deformation induced by the 2006 basel reservoir stimulation. *Geophysics*, 80(4), KS51–KS68.
- Hirose, T., Nakahara, H., & Nishimura, T. (2017). Combined use of repeated active shots and ambient noise to detect temporal changes in seismic velocity: Application to Sakurajima volcano, Japan. *Earth, Planets and Space*, 69(1), 42. <https://doi.org/10.1186/s40623-017-0613-7>
- Hotovec-Ellis, A. J., Vidale, J. E., Gombert, J., Thelen, W., & Moran, S. C. (2015). Changes in seismic velocity during the first 14 months of the 2004–2008 eruption of Mount St. Helens, Washington. *Journal of Geophysical Research: Solid Earth*, 120, 6226–6240. <https://doi.org/10.1002/2015JB012101>
- Johnson, P. A., & Jia, X. (2005). Nonlinear dynamics, granular media and dynamic earthquake triggering. *Nature*, 437(7060), 871–874.
- Judson, J., Thelen, W. A., Greenfield, T., & White, R. S. (2018). Focused seismicity triggered by flank instability on Kilauea's southwest rift zone. *Journal of Volcanology and Geothermal Research*, 353, 95–101.
- Kilburn, C. R. (2003). Multiscale fracturing as a key to forecasting volcanic eruptions. *Journal of Volcanology and Geothermal Research*, 125(3–4), 271–289. [https://doi.org/10.1016/S0377-0273\(03\)00117-3](https://doi.org/10.1016/S0377-0273(03)00117-3)
- Kilburn, C. (2012). Precursory deformation and fracture before brittle rock failure and potential application to volcanic unrest. *Journal of Geophysical Research*, 117, B02211. <https://doi.org/10.1029/2011JB008703>
- Klein, F. W. (1981). A linear gradient crustal model for south hawaii. *Bulletin of the Seismological Society of America*, 71(5), 1503–1510.
- Lengliné, O., Marsan, D., Got, J.-L., Pinel, V., Ferrazzini, V., & Okubo, P. G. (2008). Seismicity and deformation induced by magma accumulation at three basaltic volcanoes. *Journal of Geophysical Research*, 113, B12305. <https://doi.org/10.1029/2008JB005937>
- Loomis, I. (2018). Kilauea eruption abruptly slows down. *Eos*, 99. Retrieved from <https://eos.org/articles/kilauea-eruption-abruptly-slows-down> <https://doi.org/10.1029/2018EO104161>
- Mainsant, G., Larose, E., Bronnimann, C., Jongmans, D., Michoud, C., & Jaboyedoff, M. (2012). Ambient seismic noise monitoring of a clay landslide: Toward failure prediction. *Journal of Geophysical Research*, 117, F01030. <https://doi.org/10.1029/2011JF002159>
- McLeod, P., & Tait, S. (1999). The growth of dykes from magma chambers. *Journal of Volcanology and Geothermal Research*, 92(3–4), 231–245. [https://doi.org/10.1016/S0377-0273\(99\)00053-0](https://doi.org/10.1016/S0377-0273(99)00053-0)
- Mordret, A., Mikesell, T. D., Harig, C., Lipovsky, B. P., & Prieto, G. A. (2016). Monitoring southwest Greenland's ice sheet melt with ambient seismic noise. *Science Advances*, 2(5), e1501538.
- Neal, C., Brantley, S., Antolik, L., Babb, J., Burgess, M., Calles, K., et al. (2019). The 2018 rift eruption and summit collapse of Kilauea volcano. *Science*, 363(6425), 367–374.
- Obermann, A., Kraft, T., Larose, E., & Wiemer, S. (2015). Potential of ambient seismic noise techniques to monitor the St. Gallen geothermal site (Switzerland). *Journal of Geophysical Research: Solid Earth*, 120, 4301–4316. <https://doi.org/10.1002/2014JB011817>
- Olivier, G., Brenguier, F., Campillo, M., Lynch, R., & Roux, P. (2015). Bodywave reconstruction from ambient seismic noise correlations in an underground mine. *Geophysics*, 80(3), KS11–KS25.
- Olivier, G., Brenguier, F., Campillo, M., Roux, P., Shapiro, N. M., & Lynch, R. (2015). Investigation of coseismic and postseismic processes using in situ measurements of seismic velocity variations in an underground mine. *Geophysical Research Letters*, 42, 9261–9269. <https://doi.org/10.1002/2015GL065975>
- Olivier, G., Brenguier, F., de Wit, T., & Lynch, R. (2017). Monitoring the stability of tailings dam walls with ambient seismic noise. *The Leading Edge*, 36, 350a1–350a6.
- Owen, S., Segall, P., Lisowski, M., Miklius, A., Denlinger, R., & Sako, M. (2000). Rapid deformation of Kilauea Volcano: Global Positioning System measurements between 1990 and 1996. *Journal of Geophysical Research*, 105(B8), 18,983–18,998. <https://doi.org/10.1029/2000JB900109>
- Patanè, D., Barberi, G., Cocina, O., De Cori, P., & Chiarabba, C. (2006). Timereolved seismic tomography detects magma intrusions at Mount Etna. *Science*, 313(5788), 821–823.
- Peltier, A., & Bachèlery, P. (2009). A review of geophysical and geochemical data. *Journal of Volcanology and Geothermal Research*, 184(1–2), 93–108. <https://doi.org/10.1016/j.jvolgears.2008.12.008>
- Peltier, A., Ferrazzini, V., Staudacher, T., & Bachèlery, P. (2005). Imaging the dynamics of dyke propagation prior to the 2000–2003 flank eruptions at Piton de La Fournaise, Reunion Island. *Geophysical Research Letters*, 32, L22302. <https://doi.org/10.1029/2005GL023720>
- Peltier, A., Staudacher, T., Catherine, P., Ricard, L.-P., Kowalski, P., & Bachèlery, P. (2006). Subtle precursors of volcanic eruptions at Piton de la Fournaise detected by extensometers. *Geophysical Research Letters*, 33, L06315. <https://doi.org/10.1029/2005GL025495>
- Planès, T., Larose, E., Rossetto, V., & Margerin, L. (2015). Imaging multiple local changes in heterogeneous media with diffuse waves. *JASA*, 2(137), 660–667.
- Poland, M. P., Miklius, A., & Montgomery-Brown, E. K. (2014). Magma supply, storage, and transport at shield-stage hawaiian volcanoes: Chapter 5 in characteristics of hawaiian volcanoes (Tech. Rep.) Reston, VA: US Geological Survey.
- Ratdomopurbo, A., & Poupinet, G. (1995). Monitoring a temporal change of seismic velocity in a volcano: Application to the 1992 eruption of Mt. Merapi (Indonesia). *Geophysical Research Letters*, 22(7), 775–778. <https://doi.org/10.1029/95GL00302>
- Reardon, S. (2018). Hawaii volcano eruption holds clues to predicting similar events elsewhere. *Nature*, 557(7706), 477–477. <https://doi.org/10.1038/d41586-018-05206-w>
- Rivet, D., Brenguier, F., Clarke, D., Shapiro, N. M., & Peltier, A. (2014). Long-term dynamics of Piton de la Fournaise volcano from 13 years of seismic velocity change measurements and GPS observations. *Journal of Geophysical Research: Solid Earth*, 119, 7654–7666. <https://doi.org/10.1002/2014JB011307>

- Sánchez-Pastor, P., Obermann, A., & Schimmel, M. (2018). Detecting and locating precursory signals during the 2011 El Hierro, Canary Islands, submarine eruption. *Geophysical Research Letters*, *45*, 10,288–10,297. <https://doi.org/10.1029/2018GL079550>
- Schmid, A., Grasso, J. R., Clarke, D., Ferrazzini, V., Bachèlery, P., & Staudacher, T. (2012). Eruption forerunners from multiparameter monitoring and application for eruptions time predictability (Piton de la Fournaise). *Journal of Geophysical Research*, *117*, B11203. <https://doi.org/10.1029/2012JB009167>
- Scuderi, M. M., Marone, C., Tinti, E., Di Stefano, G., & Collettini, C. (2016). Precursory changes in seismic velocity for the spectrum of earthquake failure modes. *Nature Geoscience*, *9*(9), 695–700. <https://doi.org/10.1038/ngeo2775>
- Sens-Schönfelder, C., Pomponi, E., & Peltier, A. (2014). Dynamics of Piton de la Fournaise volcano observed by passive image interferometry with multiple references. *Journal of Volcanology and Geothermal Research*, *276*, 32–45. <https://doi.org/10.1016/J.JVOLGEORES.2014.02.012>
- Sens-Schönfelder, C., & Wegler, U. (2006). Passive image interferometry and seasonal variations of seismic velocities at Merapi Volcano, Indonesia. *Geophysical Research Letters*, *33*, L21302. <https://doi.org/10.1029/2006GL027797>
- Surono, J. P., Pallister, J., Boichu, M., Buongiorno, M. F., Budisantoso, A., Costa, F., et al. (2012). The 2010 explosive eruption of Java's Merapi volcano—A '100-year' event. *Journal of Volcanology and Geothermal Research*, *241-242*, 121–135. <https://doi.org/10.1016/J.JVOLGEORES.2012.06.018>
- Tait, S., Jaupart, C., & Vergnolle, S. (1989). Pressure, gas content and eruption periodicity of a shallow, crystallising magma chamber. *Earth and Planetary Science Letters*, *92*(1), 107–123. [https://doi.org/10.1016/0012-821X\(89\)90025-3](https://doi.org/10.1016/0012-821X(89)90025-3)
- Toda, S., Stein, R. S., Sevilgen, V., & Lin, J. (2011). Coulomb 3.3 graphic-rich deformation and stress-change software for earthquake, tectonic, and volcano research and teaching-user guide (Tech. Rep.) Reston: US Geological Survey.
- Voight, B. (1988). A method for prediction of volcanic eruptions. *Nature*, *332*(6160), 125–130. <https://doi.org/10.1038/332125a0>
- Wegler, U., Lühr, B.-G., Snieder, R., & Ratdomopurbo, A. (2006). Increase of shear wave velocity before the 1998 eruption of Merapi volcano (Indonesia). *Geophysical Research Letters*, *33*, L09303. <https://doi.org/10.1029/2006GL025928>
- Wells, D. L., & Coppersmith, K. J. (1994). New empirical relationships among magnitude, rupture length, rupture width, rupture area, and surface displacement. *Bulletin of the seismological Society of America*, *84*(4), 974–1002.
- Zhan, Z., Tsai, V. C., & Clayton, R. W. (2013). Spurious velocity changes caused by temporal variations in ambient noise frequency content. *Geophysical Journal International*, *194*(3), 1574–1581. <https://doi.org/10.1093/gji/ggt170>